




Original Research

Accuracy of Preoperative Breast MRI Versus Conventional Imaging in Measuring Pathologic Extent of Invasive Lobular Carcinoma

Keegan K. Hovis, MD,¹ Janie M. Lee, MD,^{1,2} Daniel S. Hippe, MS,¹
Hannah Linden, MD,^{2,3} Meghan R. Flanagan, MD,^{2,4} Mark R. Kilgore, MD,^{2,5}
Janis Yee, MD,¹ Savannah C. Partridge, PhD,^{1,2} Habib Rahbar, MD^{1,2,*} 

¹University of Washington School of Medicine, Department of Radiology, Seattle, WA, USA; ²Seattle Cancer Care Alliance, Seattle, WA, USA; ³University of Washington School of Medicine, Department of Medical Oncology, Seattle, WA, USA; ⁴University of Washington School of Medicine, Department of Surgery, Seattle, WA, USA; ⁵University of Washington School of Medicine, Department of Laboratory Medicine and Pathology, Seattle, WA, USA

*Address correspondence to H.R. (e-mail: hrahbar@uw.edu)

Abstract

Objective: To determine whether invasive lobular carcinoma (ILC) extent is more accurately depicted with preoperative MRI (pMRI) than conventional imaging (mammography and/or ultrasound).

Methods: After IRB approval, we retrospectively identified women with pMRIs (February 2005 to January 2014) to evaluate pure ILC excluding those with ipsilateral pMRI BI-RADS 4 or 5 findings or who had neoadjuvant chemotherapy. Agreement between imaging and pathology sizes was summarized using Bland-Altman plots, absolute and percent differences, and the intraclass correlation coefficient (ICC). Rates of underestimation and overestimation were evaluated and their associations with clinical features were explored.

Results: Among the 56 women included, pMRI demonstrated better agreement with pathology than conventional imaging by mean absolute difference (1.6 mm versus -7.8 mm, $P < 0.001$), percent difference (10.3% versus -16.4%, $P < 0.001$), and ICC (0.88 versus 0.61, $P = 0.019$). Conventional imaging more frequently underestimated ILC span than pMRI using a 5 mm difference threshold (24/56 (43%) versus 10/56 (18%), $P < 0.001$), a 25% threshold (19/53 (36%) versus 10/53 (19%), $P = 0.035$), and T category change (17/56 (30%) versus 7/56 (13%), $P = 0.006$). Imaging–pathology size concordance was greater for MRI-described solitary masses than other lesions for both MRI and conventional imaging ($P < 0.05$). Variability of conventional imaging was lower for patients \geq the median age of 62 years than for younger patients (SD: 12 mm versus 22 mm, $P = 0.012$).

Conclusion: MRI depicts pure ILC size more accurately than conventional imaging and may have particular value for younger women.

Key words: breast MRI; invasive lobular carcinoma; breast cancer staging; pathologic extent of disease; mammography; ultrasound.

Key Messages

- MRI depicts invasive lobular carcinoma (ILC) pathologic size more accurately than conventional imaging, which more often underestimates ILC size and the T category of stage.
- ILC presenting as a solitary mass on MRI had greater imaging-to-pathology size concordance than those presenting as multiple masses, non-mass enhancement (NME), or mixed mass and NME.
- Accuracy of conventional imaging for ILC span was better in women aged 62 years (the median age) and older than in those younger than 62 years, while MRI accuracy was not affected by age.

Introduction

Invasive lobular carcinoma (ILC) is the second most common histologic type of invasive breast cancer and accounts for 10%–15% of all invasive breast malignancies, and its incidence is steadily increasing (1). Its histopathologic and molecular features, typically including loss of E-cadherin, estrogen receptor positivity, a low-to-moderate proliferation index, and its discrete metastatic profile have led many to consider it a distinct disease from its invasive ductal counterpart (2). From an imaging standpoint, ILC can be particularly challenging to detect by conventional imaging with mammography and/or ultrasound due to its infiltrative and poorly cohesive growth pattern and minimal surrounding desmoplastic reaction (3,4). The sensitivity of mammography in ILC detection is reported as 57%–81%, compared to sensitivity benchmarks of 87.8% for diagnostic mammography (5) and 86.9% for screening mammography (6) for all breast cancers. The sensitivity of ultrasound to detect ILC has been reported to have a slightly higher range of 68%–98% (7), though it should be noted that there are no clear sensitivity benchmarks for this modality for women with all mammographic densities. The wide ranges of reported accuracy in the depiction of ILC by conventional imaging are likely due to the propensity of ILC to be of equal or lower density than adjacent normal fibroglandular tissue, ill-defined mass shape and margins, frequent presentation as architectural distortion or a one-view finding, and lack of associated suspicious calcifications when compared to invasive ductal carcinoma (IDC), resulting in both over- and underestimation of disease extent (7).

Preoperative breast MRI is now commonly used to more accurately determine, compared to conventional mammogram and/or ultrasound alone, the extent of newly diagnosed breast cancer. Due to the challenging imaging presentation of ILC, several medical societies, including the American Society of Breast Surgeons, the National Comprehensive Cancer Network, the European Society of Breast Cancer Specialists, and the European Society of Breast Imaging, recommend

particular consideration of preoperative MRI for patients with ILC. Although the sensitivity of MRI for ILC detection is higher than mammography and ultrasound (range: 83%–100%), data on the accuracy of MRI to determine maximal ILC span are mixed, possibly owing to variable MRI technique and methodology (8–10). Furthermore, because ILC is often associated with multifocal cancers, some of which have mixed lobular and ductal phenotypes, it can be challenging to determine whether imaging overestimations and underestimations of ILC described in the literature are due to false-positive findings on MRI, presence of additional ductal-phenotype breast carcinoma, differences in how total span is reported on imaging (often including skip areas of normal tissue) versus pathology, or a truly inaccurate imaging depiction of the tumor (11).

Accordingly, we sought to evaluate the relative accuracy of MRI versus conventional imaging (mammography and/or ultrasound) to determine the final pathologic span of pure ILC, defined as an ILC without associated ductal carcinoma in situ (DCIS) or IDC, at a single-institution academic center. Because MRI often identifies additional suspicious non-contiguous findings that may be reported with the index malignancy as a single maximal span, we excluded ILC lesions with additional non-contiguous suspicious areas of enhancement in order to maximize the accuracy of imaging versus pathology comparisons.

Methods**Study Design**

We performed a retrospective analysis of a clinical MRI database linked to institutional pathology outcomes. This Health Insurance Portability and Accountability Act-compliant study was approved by our institutional review board, which waived the need for informed consent. We identified all patients who underwent preoperative MRI to further evaluate a newly diagnosed ILC on core-needle biopsy from February 2005 to January 2014. All preoperative MRIs were performed within 3 months after a core-needle biopsy diagnosis of ILC and before primary surgical treatment. A Consolidated Standards of Reporting Trials flow diagram describing inclusion and exclusion of subjects is provided in Figure 1. Core-needle biopsies that included coexisting DCIS or IDC were excluded, as were MRIs with significant technical issues or additional Breast Imaging Reporting and Data System (BI-RADS) (12) category 0, 3, 4, or 5 lesions that could indicate multifocality or multicentricity. Finally, women who underwent neoadjuvant chemotherapy prior to surgery, had a final surgical result including IDC or DCIS (rather than pure ILC), or did not have a final surgical pathology report in our system were also excluded. It should be noted that all patients in this study were included in a separate paper on clinical factors that can determine the performance of preoperative MRI to find additional disease (13). The methodology of that paper was distinct, as it included all types of

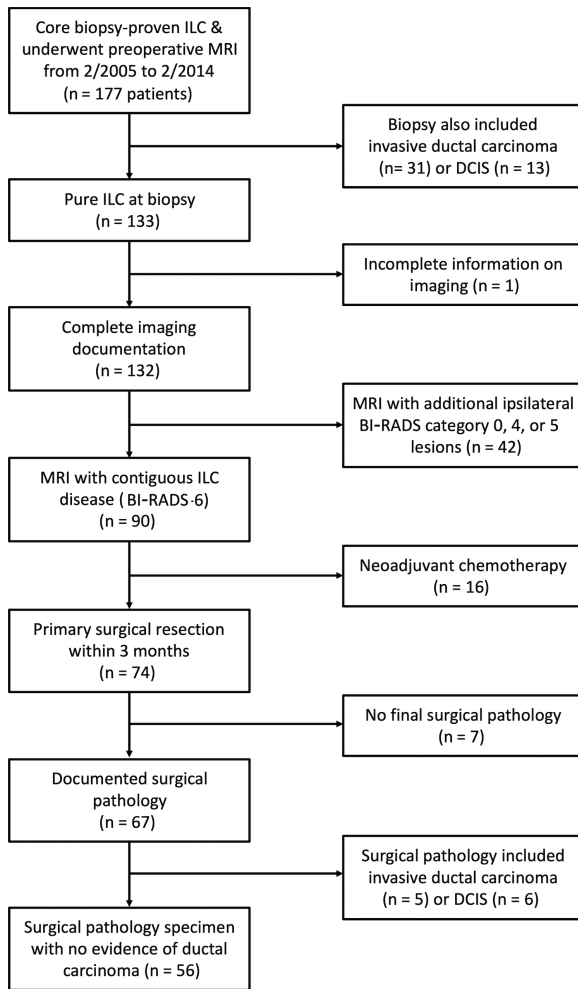


Figure 1. Consolidated Standards of Reporting Trials diagram summarizing patients included in the study. Abbreviations: DCIS, ductal carcinoma in situ; ILC, invasive lobular carcinoma.

breast cancers (not limited to ILC) and did not evaluate accuracy of MRI to depict pathologic span of disease.

MRI Acquisition

All breast MRIs were performed in accordance with the American College of Radiology Breast MRI Accreditation Program standards. Prior to 2010, exams were performed on a 1.5T scanner (LX, GE Healthcare, Waukesha, WI). From January 2010 to January 2014, MRIs were performed on a 3T scanner (Achieva Tx, Philips Healthcare, Best, the Netherlands). All scans used a dedicated breast coil and each protocol included bilateral acquisition of a pre-contrast, fat-suppressed, T2-weighted, fast-spin echo sequence followed by a T1-weighted dynamic contrast-enhanced sequence with one pre-contrast and at least three post-contrast, fat-suppressed, 3D fast-gradient echo acquisitions. K-space centering for initial post-contrast acquisitions was between 90 and 120 seconds after contrast administration, and final delayed acquisitions were centered between 4.5 and 7.5

minutes after contrast administration. Gadolinium contrast agent (before November 2010: Omniscan, GE Healthcare, Waukesha, WI; from November 2010: ProHance, Bracco Diagnostics, Princeton, NJ) was power injected (0.1 mmol/kg at 2 ml/s) followed by a 20 ml saline flush.

Patient and Tumor Features

Patient characteristics were abstracted from the electronic medical record, including patient age, race, background parenchymal enhancement (BPE), and breast density. Breast density was divided into non-dense breasts (almost entirely fatty (BI-RADS category a) and scattered fibroglandular densities (category b)) and dense breasts (heterogeneously dense (category c) and extremely dense (category d)). Maximal size on conventional imaging (mammography and/or ultrasound) and MRI was abstracted from radiology reports. A single largest size for conventional imaging was reported rather than individual span for mammography and ultrasound because our conventional imaging reports provided only a largest span based on those two modalities rather than describing the spans for each modality independently. Lesion type on MRI (mass, multiple similar-appearing masses, non-mass enhancement (NME), or mixed mass/es and NME) and conventional imaging (mass or focal asymmetry without calcifications, architectural distortion, pure calcifications, or mixed mass and calcifications) was also recorded. Of note, all lesions included in the study were categorized on MRI as BI-RADS category 6, indicating that even when multiple masses or mixed mass/es and NME were present, their proximity to the index mass (typically ≤ 2 cm edge to edge) and appearance allowed for the finding to be considered a single lesion. In all MRI cases, the single largest dimension recorded for that BI-RADS category 6 lesion was utilized. In 5 women for whom no maximal mammography or ultrasound size was described in the radiology report, retrospective measurement of maximal size was performed by a study radiologist (H.R., 10 years of post-residency breast imaging experience) blinded to the MRI and final pathology span. Maximum contiguous pathologic size, the presence of associated lobular carcinoma in situ (LCIS), T category of the stage (14), Nottingham grade, and immunohistochemical markers (estrogen receptor, progesterone receptor, and HER2) were extracted from pathology reports. Finally, surgical outcomes, including initial surgery approach (mastectomy versus breast conservation therapy) and any subsequent re-excisions were obtained from the electronic medical record.

Maximal MRI lesion size and conventional imaging size were compared to the maximal ILC span recorded on the surgical pathology reports. Underestimation and overestimation by conventional imaging versus MRI were evaluated using multiple thresholds: (1) absolute size difference of ± 5 mm; (2) relative size difference of $\pm 25\%$; and (3) whether size difference led to a change in the T category of the stage. These thresholds were chosen because 5 mm is the most widely accepted threshold to determine absolute concordance between

imaging and pathologic size in breast cancers (15–17), and 25% was found, in a prior study, to best correlate with the 5 mm cutoff but also provide a relative concordance evaluation, taking into account tumor size (18). The difference between MRI and pathologic size was then compared to the size difference between conventional imaging and pathology in order to evaluate whether MRI more accurately depicts the disease extent of ILC.

Statistical Analysis

Absolute and percent differences in ILC span on imaging and pathology were summarized graphically using Bland-Altman plots. Mean differences with pathology were tested using paired *t*-tests. Measurement variability was summarized using the standard deviation of differences (SDD) between imaging and pathology. Overall agreement with pathology was summarized using the intraclass correlation coefficient (ICC). Classifications of discordances by each modality based on ± 5 mm and $\pm 25\%$ thresholds were compared using the sign test. The T category was compared between imaging and pathology using the Wilcoxon signed-rank test. The mean difference and SDD were compared between clinical subgroups using Welch's *t*-test and the Fligner-Killeen test, respectively. All statistical calculations were conducted with the statistical computing language R (version 4.0.0; R Foundation for Statistical Computing, Vienna, Austria). Two-sided tests were used throughout, with statistical significance defined as $P < 0.05$.

Results

Patient and Lesion Features

A total of 56 patients with ILC met the study criteria. Patient, tumor, and imaging characteristics are summarized in Table 1. The most common conventional imaging findings were masses or focal asymmetries without calcifications (37/56; 66.1%) and architectural distortion (8/56; 14.3%). Most women had scattered fibroglandular densities (16/56; 28.6%) or heterogeneously dense (34/56; 60.7%) breast density on mammography, and minimal (23/56; 41.1%) or mild (20/56; 35.7%) BPE on MRI. ILC lesions were described on MRI most frequently as a single mass (26/56; 46.4%), followed by NME (13/56; 23.2%), mixed mass and NME (8/56; 14.3%), multiple similar-appearing masses (6/56; 10.7%), and no enhancement at the site (3/56; 5.4%). No lesions were described as a focus of enhancement. Of the 3 patients with no MRI enhancement at the site of biopsy, 2 had no ILC on final pathology while 1 had an ILC tumor spanning 30 mm at surgery. Most ILCs were also accompanied by LCIS (41/56; 73.2%).

Of the 56 women, 38/56 (68%) underwent breast conservation and the remaining 18/56 (32%) underwent mastectomy. Of the 38 women for whom breast conservation was performed, 4 underwent a single re-excision due to positive margins (4/38; 11%; 95% confidence interval (CI): 3%–25%); none were converted to mastectomy.

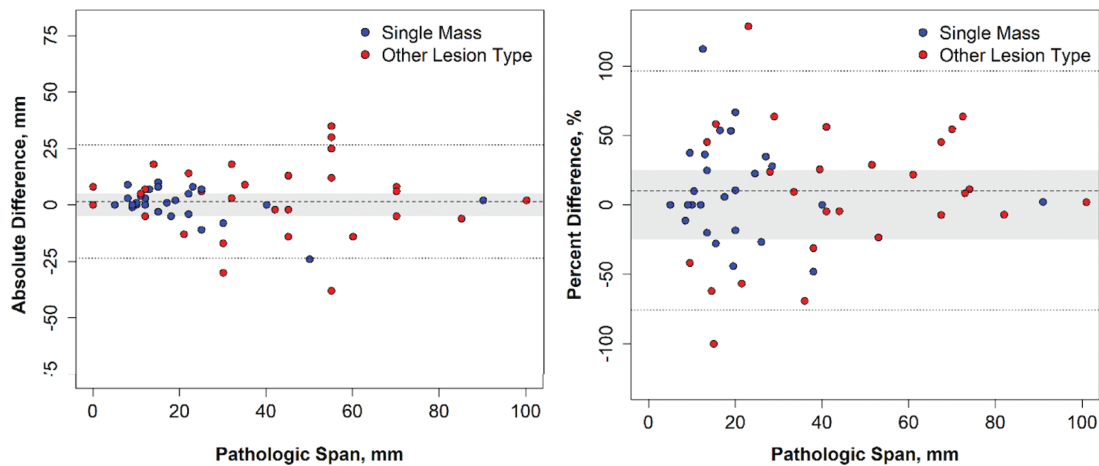
Table 1. Patient Characteristics ($N = 56$)

Variable	n/N (%)
Mean age, years (range)	62 (33–86)
Race	
Caucasian	47/55 (85.5)
Other	8/55 (14.5)
Breast density	
Almost entirely fatty	2/56 (3.6)
Scattered fibroglandular densities	16/56 (28.6)
Heterogeneously dense	34/56 (60.7)
Extremely dense	4/56 (7.1)
Conventional imaging lesion type	
Mass or focal asymmetry without calcifications	37/56 (66.1)
Architectural distortion	8/56 (14.3)
Calcifications without mass	7/56 (12.5)
Calcifications with mass	4/56 (7.1)
MRI lesion type	
Single mass	26/56 (46.4)
Multiple masses	6/56 (10.7)
Non-mass enhancement	13/56 (23.2)
Mass + non-mass enhancement	8/56 (14.3)
None	3/56 (5.4)
Background parenchymal enhancement	
Minimal	23/56 (41.1)
Mild	20/56 (35.7)
Moderate	8/56 (14.3)
Marked	5/56 (8.9)
T category of stage	
T1	24/56 (42.9)
T2	20/56 (35.7)
T3	12/56 (21.4)
Nottingham grade	
1	13/53 (24.5)
2	32/53 (60.4)
3	8/53 (15.1)
Estrogen receptor status	
Positive	54/56 (96.4)
Negative	2/56 (3.6)
Progesterone receptor status	
Positive	41/56 (73.2)
Negative	15/56 (26.8)
HER2 status	
Positive	2/54 (3.7)
Negative	51/54 (94.4)
Equivocal/indeterminate	1/54 (1.9)
Lobular carcinoma in situ component	
Present	41/56 (73.2)
Absent	15/56 (26.8)

Comparison of Imaging Span With Pathology Span

The distribution of absolute and percent size differences of MRI and conventional imaging versus pathology are described in the Bland-Altman plots in Figure 2. The span of ILC ranged from 0 to 100 mm (median: 23 mm) on surgical pathology, 0 to 102 mm (median: 23 mm) on MRI, and 5 to 80 mm (median: 15 mm) on conventional imaging. On average, ILC span measured by MRI was 1.6 mm (95% CI: –1.8–4.9 mm)

MRI vs. Pathology



Conventional Imaging vs. Pathology

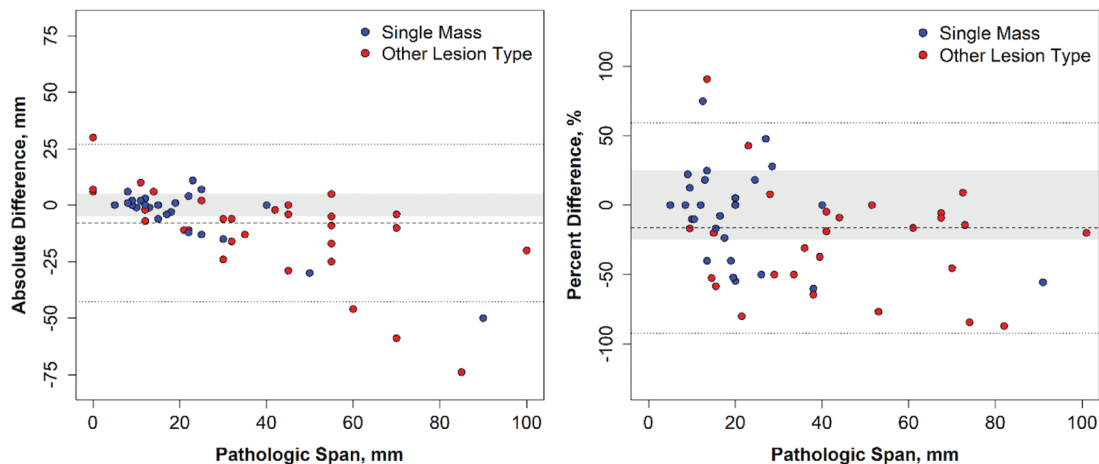


Figure 2. Comparison of invasive lobular carcinoma lesion span on imaging versus pathology. Measurement results from MRI are shown on the top panel, and measurement results from conventional imaging with mammography and US are shown on the bottom panel. The left panels are Bland-Altman plots with the absolute difference between lesion span on imaging and pathology versus span on pathology. The mean absolute difference is shown by the dashed line, and limits of agreement are shown by the dotted lines, with the gray zone indicating differences of ± 5 mm. The right panels are Bland-Altman plots with the percent difference between lesion span on imaging and pathology versus span on pathology. The mean percent difference and limits of agreement based on percent difference are shown by the dashed and dotted lines, respectively, and the gray zone indicates differences of $\pm 25\%$. There were 3 cases with spans of zero on pathology that are not included on the right panels.

or 10.3% (95% CI: -1.6 – 22.1%) larger than pathologic span, neither of which were statistically significant (Table 2). In contrast, conventional imaging significantly underestimated pathologic span by 7.8 mm (95% CI: 3.2 – 12.5 mm, $P < 0.001$ compared to MRI) or 16.4% (95% CI: 5.9% – 26.8% , $P < 0.001$ compared to MRI). Span of ILC measured by MRI also had significantly higher overall agreement with pathologic span than ILC span measured by conventional imaging (ICC: 0.88 versus 0.61, $P = 0.019$).

Frequency of Overestimation and Underestimation With MRI and Conventional Imaging

MRI demonstrated no significant predilection to overestimate versus underestimate ILC span. Specifically, when evaluating concordance using the ± 5 mm threshold, 10/56 (18%) were underestimated while 20/56 (36%) were overestimated on MRI ($P = 0.099$) (Table 3). Similarly, of the 53

Table 2. Comparison of Imaging and Pathology Measurements of the Span of ILC

Modality	ILC Span, Mean ± SD		Absolute Difference, mm			Relative Difference, %			Agreement	
	Imaging	Path	Mean (95% CI)	P-value ^a	LoA	Mean (95% CI)	P-value ^a	LoA	ICC (95% CI)	
MRI	32 ± 27	31 ± 24	1.6 (-1.8, 4.9)	0.36	-24, 27	10.3 (-1.6, 22.1)	0.088	-76, 96	0.88 (0.80, 0.93)	
MG/US	23 ± 17	31 ± 24	-7.8 (-12.5, -3.2)	0.001	-43, 27	-16.4 (-26.8, -5.9)	0.003	-92, 59	0.61 (0.38, 0.76)	

Abbreviations: CI, confidence interval; ICC, intraclass correlation coefficient; ILC, invasive lobular carcinoma; LoA, limits of agreement; MG, mammography.

^aTest of mean difference = 0 using paired *t*-test.

Table 3. Over- and Underestimation of the Span of Invasive Lobular Carcinoma (ILC) on MRI and Conventional Imaging

Criteria	MRI				Conventional Imaging			
	ILC Span Compared to Pathology n/N (%)		P-value ^b		ILC Span Compared to Pathology n/N (%)		P-value ^b	
	Overestimated	Underestimated	Overestimated	Underestimated	Overestimated	Underestimated	Overestimated	Underestimated
Difference >5 mm	20/56 (35.7)	10/56 (17.9)	0.099	8/56 (14.3)	24/56 (42.9)	0.007		
Difference >25% ^a	18/53 (34.0)	10/53 (18.9)	0.18	5/53 (9.4)	19/53 (35.8)	0.007		
T category of stage difference			0.46			<0.001		
1 level	5/56 (8.9)	6/56 (10.7)	-	2/56 (3.6)	14/56 (25.0)	-		
2 levels	0/56 (0.0)	1/56 (1.8)	-	0/56 (0.0)	3/56 (5.4)	-		

^a53 of 56 lesions had non-zero size on pathology and were included when calculating relative differences in maximal size on imaging.

^bTest of difference rates of overestimation and underestimation using the sign test or Wilcoxon signed-rank test.

lesions with non-zero size on pathology, 10/53 (19%) were underestimated and 18/53 (34%) overestimated disease by at least 25% on MRI ($P = 0.18$).

However, using conventional imaging, ILC lesions were more likely to be underestimated. Using the ± 5 mm threshold, ILC span was underestimated in 24/56 (43%) lesions and overestimated in 8/56 (14%) ($P = 0.007$). Similarly, of the 53 lesions with non-zero size on pathology, ILC span was underestimated in 19/53 (36%) and overestimated in 5/53 (9%) by at least 25% ($P = 0.007$) on conventional imaging.

When evaluating concordance using the T category, MRI and pathology agreed in 44/56 (79%) cases. Of the 12 disagreements, similar numbers were underestimated and overestimated (7 and 5, respectively, $P = 0.46$) (Table 3). T category was less concordant between conventional imaging and pathology in 37/56 (66%), and there were more underestimations of T category than overestimations (17/56 (30%) versus 2/56 (4%), $P < 0.001$).

Overall, conventional imaging underestimated ILC span more than MRI according to any of the three criteria: the ± 5 mm threshold (24/56 (43%) versus 10/56 (18%), $P < 0.001$), the $\pm 25\%$ threshold (19/53 (36%) versus 10/53 (19%), $P = 0.035$), and a change in T category (17/56 (30%) versus 7/56 (13%), $P = 0.006$). Examples of ILC pathology span and concordance with MRI versus conventional imaging are provided in Figures 3–5.

Factors Affecting Imaging Accuracy of ILC Span

A subgroup analysis was performed to determine whether a number of clinical variables would impact the accuracy of MRI versus pathologic size (Supplemental Table 1) and mammography/ultrasound versus pathologic size (Supplemental Table 2). Solitary masses, as described on MRI, were associated with less measurement variability than other lesion types (multiple masses, NME, or both) for both MRI (SDD: 7 mm versus 16 mm, $P = 0.002$) and conventional imaging (SDD: 12 mm versus 21 mm $P = 0.016$). No conventional imaging feature (eg, architectural distortion, mass and/or focal asymmetry, or calcifications) was associated with less measurement variability for either MRI or conventional imaging. Lesions in patients aged ≥ 62 years (median age) also had significantly less measurement variability on conventional imaging compared to younger patients (SDD: 12 mm versus 22 mm, $P = 0.012$); however, age was not found to impact measurement variability for MRI. Of note, younger patients (<62 years) were more likely to have dense breasts (24/28 (86%) versus 14/28 (50%), $P = 0.009$) and less likely to have a solitary mass on MRI (7/28 (25%) versus 19/28 (68%), $P = 0.003$) than older patients.

Discussion

In this study of pure ILC, we found that MRI is more likely to demonstrate a maximal span that is concordant with final surgical pathology size compared to conventional imaging

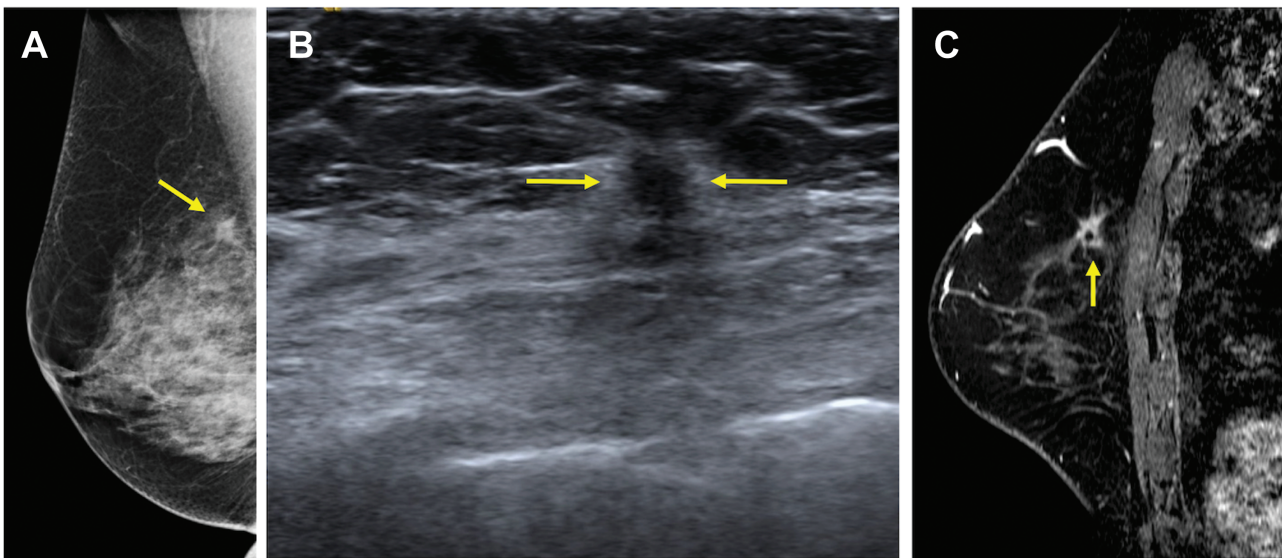


Figure 3. 70-year-old woman who presented with a screening-detected mass in the right breast in the upper inner quadrant shown to be an invasive lobular carcinoma (ILC) (Nottingham grade II, estrogen and progesterone receptor positive, HER2 negative) with associated lobular carcinoma in situ on core-needle biopsy, which serves as an example of concordant depiction of the span of ILC on both conventional imaging and MRI when compared to final pathology. **A:** Diagnostic mediolateral oblique mammogram demonstrated an irregular mass with spiculated margins measuring 12 mm (arrow). **B:** Targeted US depicted a round mass with indistinct margins measuring 8 mm (arrows). **C:** MRI performed after core-needle biopsy and prior to surgery depicted the finding as an irregular mass with spiculated margins measuring 12 mm and containing a biopsy marker clip (arrow). Final pathologic size was 12 mm on mastectomy, which was concordant with maximal size on conventional imaging and MRI.

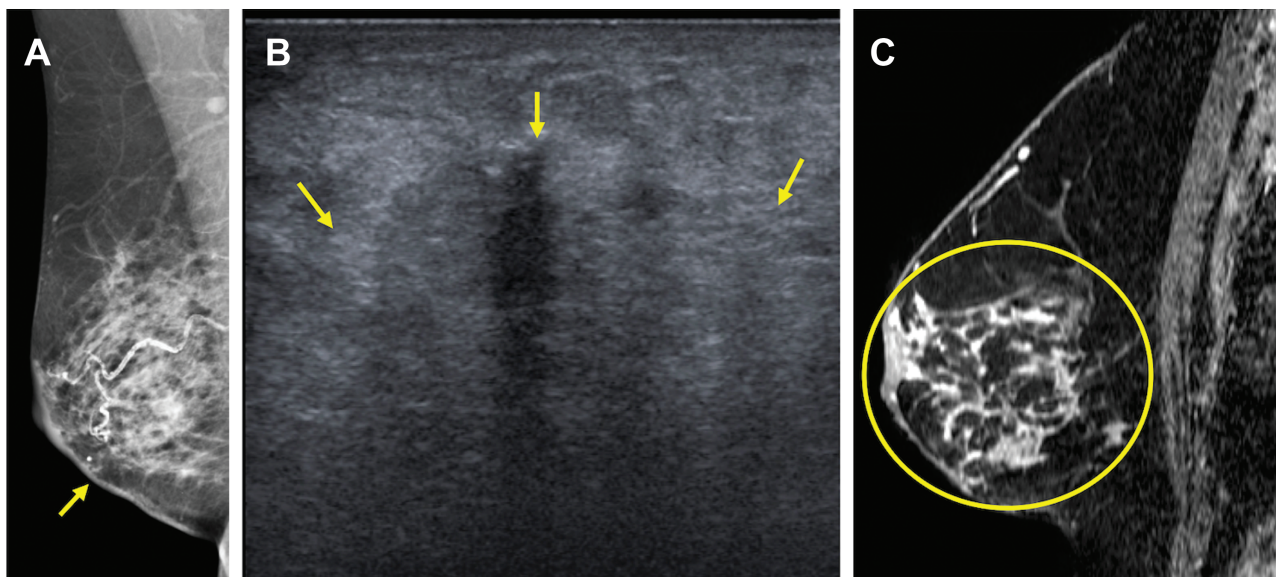


Figure 4. 70-year-old woman who presented with a self-detected mass in the right lower inner quadrant diagnosed on core-needle biopsy as invasive lobular carcinoma (ILC) (Nottingham grade 1, estrogen and progesterone receptor positive, HER2-negative) with associated lobular carcinoma in situ, which serves as an example of concordant estimation of the span of ILC on MRI with underestimation on conventional imaging. **A:** Diagnostic mediolateral oblique mammogram demonstrated skin thickening at the site of concern (arrow), but no definite mass. **B:** Targeted US demonstrated an ill-defined irregular-shaped mass with indistinct margins (arrows) that was difficult to measure but estimated to span 40 mm. **C:** MRI performed after biopsy demonstrated a total span of 92 mm of non-mass enhancement (circle) involving the lower inner and lower outer quadrants. Final pathologic size was 90 mm on mastectomy. Conventional imaging underestimated size based on the 5 mm, 25%, and T category of stage thresholds, while MRI was accurate using all three thresholds.

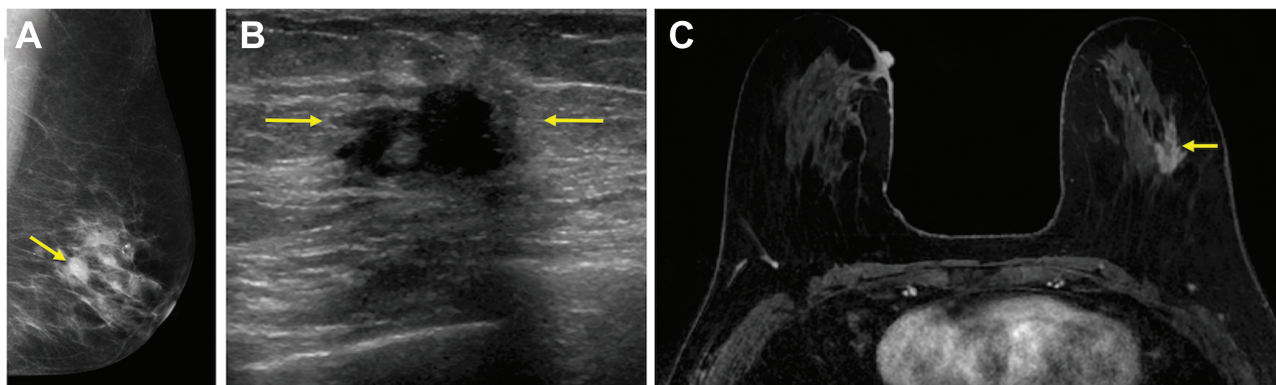


Figure 5. 66-year-old woman who presented with a screening-detected mass in the left breast in the upper outer quadrant diagnosed on core-needle biopsy as invasive lobular carcinoma (ILC) (Nottingham grade II, estrogen and progesterone receptor positive, HER2-negative) with associated lobular carcinoma in situ, which serves as an example of overestimation of an ILC span on MRI with concordant depiction of span on conventional imaging. **A:** Diagnostic mediolateral oblique mammogram demonstrated an irregular-shaped mass with spiculated margins measuring 15 mm (arrow). **B:** Targeted US depicted an irregular mass with indistinct margins also measuring 15 mm (arrows). **C:** MRI performed after core-needle biopsy depicted the finding as an irregular mass with spiculated margins measuring 25 mm (arrow). Final pathologic size was 15 mm on mastectomy. MRI overestimated size by the 5 mm, 25%, and T category of stage thresholds, while conventional imaging was concordant using all three thresholds.

with mammography and/or ultrasound. We also demonstrated that conventional imaging tends to underestimate the size of ILC, whether using a 5 mm absolute threshold, a 25% threshold, or a change in the T category of stage. Importantly, conventional imaging underestimated the T category of ILC in 30% of cases, which may have implications for treatment

planning and clinical trial eligibility. Finally, we demonstrated that single mass lesions on MRI were more likely to be concordant with pathology than other lesion types.

Our study adds to the existing body of literature that suggests MRI depicts ILC span more accurately than conventional imaging with mammography and ultrasound. The

potential value of MRI to provide a more accurate span of ILC prior to surgery has been reported in multiple single-institution studies (8–10,19), with a meta-analysis of six studies estimating a correlation coefficient of 0.89 (95% CI: 0.84–0.93) when comparing MRI and pathologic sizes (11). Our study also confirms findings from prior investigators, who demonstrated that conventional imaging with mammography and/or ultrasound can significantly underestimate the span of ILC (9,20–25). Our study demonstrated that conventional imaging underestimates ILC by an average of 7.8 mm (16%), with significant predilection for underestimation using thresholds of ± 5 mm and $\pm 25\%$ of size. Similar to our results, ultrasound underestimated ILC tumor size by an average of 27.2% in one prior study (24) and had a mean size underestimation of 10 mm in another (21), while mammography under-staged 35%–48% of ILC cases out of 42 tumors in a third study (23). Further, Mann et al demonstrated that out of 68 ILC tumors, 19% were mammographically occult, and another 54% were underestimated by more than 10 mm on mammography (9).

Our study demonstrated that MRI more often overestimated (34%–36%) than underestimated (18%–19%) ILC span using 5 mm and 25% thresholds, though this difference was not statistically significant. Lai et al also used a cutoff of $\pm 25\%$ and found that MRI had a propensity toward overestimation, with fairly similar rates when compared to our study (overestimation in 27.3% versus underestimation in 13.6%) (18). However, direct comparison of our study with many of the other prior studies is challenging due to widely varying methodologies, including inclusion of multifocal and/or multicentric ILC (8–10,26–29), presence of coexisting DCIS (9), and inconsistent metrics as to what constituted imaging-to-pathology span concordance (9,26–29). For example, two different studies used a more lenient absolute threshold of 10 mm and found underestimation with MRI in 13.9%–15.9% and overestimation in 10.1%–11.1% (9,26), while another study used an extremely stringent threshold of 1 mm and demonstrated underestimation in 59.1% and overestimation in 34.1% (27). Furthermore, two other studies described overestimation and underestimation using accuracy of MRI to correctly identify multifocal and multicentric disease (28,29), which was excluded from this study.

A clinically important aspect of this study was assessment of discrepancies in the T category between imaging and final pathology. We found that MRI had similar underestimation and overestimation rates of the T category, while conventional imaging underestimated the T category in 30% of cases, twice as often as MRI. Since T1 tumors cannot be underestimated and T3 tumors cannot be overestimated (with respect to absolute size), the use of T category agreement between imaging and pathology weights this measure of accuracy toward tumors in the study population that are close to the 2 cm threshold for the T2 category and the 5 cm threshold for the T3 category. Accuracy of the T2 and T3 categories is clinically relevant for both medical and surgical oncology

treatment planning, since such ILC tumors have improved breast conservation surgery outcomes after neoadjuvant chemotherapy (30,31). The T category of stage is also often an important clinical trial inclusion criterion. Furthermore, although appropriateness for primary breast conservation surgery versus mastectomy is dependent on tumor size to breast size ratio and tumor biology, breast conservation is most commonly performed for tumors smaller than 5 cm, which corresponds to T1 and T2 categories (32,33). Thus, our study suggests particular value for preoperative MRI in women with ILC for whom neoadjuvant chemotherapy and/or breast conservation therapy are being considered.

We also explored the effect of various clinical, pathologic, and imaging variables on imaging-to-pathology size concordance. Interestingly, ILC presentation as a single mass on MRI was associated with greater accuracy for both MRI and conventional imaging span. To our knowledge, this represents a novel analysis that has not been previously reported and suggests that ILC cases that present as NME or multiple masses are more likely to be challenging for accurate preoperative localization. We did not find the presence of LCIS to be associated with overestimation on MRI, which is in contrast to at least one prior report (9). This lack of association may be due to the fact that LCIS was present in the majority (73.2%) of our cases, possibly representing a difference in pathology reporting style across institutions, especially in cases of atypia (34). Last, we found that variability between conventional imaging and pathology spans was less variable in women aged 62 years and older. This association was likely driven in part by the fact that younger patients were more likely to have dense breasts, and mammographic density is known to independently and adversely affect performance due to its ability to mask cancers. Furthermore, we found that older women were more likely to have a solitary mass on MRI than younger patients, which also likely decreased variability of conventional imaging span relative to pathologic size. Still, a more judicious approach for obtaining MRI might be considered for older women, especially in those with less dense breasts and significant comorbidities.

In this study, we demonstrate a re-excision rate of 11% for ILC with preoperative MRI, which compares favorably to recently published rates of up to 32.4% (102/314) at a similar academic institution (35). However, because we had no control cohort of women who did not receive MRI, we could not directly determine whether MRI itself is associated with improved surgical outcomes. A recent meta-analysis of 766 patients with ILC across 19 studies indicated there were fewer re-excisions after initial breast conservation in the MRI cohorts than in the no-MRI cohorts (10.9% versus 18.0%, $P = 0.031$) (36). The fact that the re-excision rate from this study aligns well with that meta-analysis further strengthens the conclusion that preoperative MRI can provide particular benefit in this population.

Our study has several limitations. Patients with multifocal, multicentric, or contralateral disease were not included.

While this was done to allow for more accurate comparison of imaging to pathology span, these scenarios are particularly common in ILC and may limit the generalizability of our findings. During the study period, subtypes of pleomorphic ILC and LCIS were not consistently reported, and it is possible that such subtypes are more likely to impact MRI estimations. We also excluded preoperative MRIs for women who underwent neoadjuvant chemotherapy; thus, our findings cannot be generalized to assume post-neoadjuvant MRI for surgical planning can provide better depiction of residual disease than conventional imaging. We were not able to separately assess performance of ultrasound versus mammography. Finally, our study pre-dated the use of digital breast tomosynthesis (DBT) for diagnostic applications at our institution, and it is possible that DBT could improve conventional imaging performance.

Conclusions

In conclusion, our study found that preoperative MRI had superior absolute agreement with pathologic size compared to conventional imaging with mammography and/or ultrasound. Conventional imaging consistently underestimated ILC extent, whether evaluated in absolute terms or using various thresholds. We also found that the presence of a single mass on MRI was associated with a greater likelihood of imaging-to-pathology size agreement compared with NME or multiple masses. Our results suggest that preoperative MRI could provide particular value for surgical planning of ILC by allowing better depiction of disease, particularly for women who are found to have a single mass on MRI, are younger than 62 years of age, and are considering breast conservation therapy. Future prospective or randomly assigned studies with no-MRI control cohorts specifically for women with ILC are needed to evaluate whether this improved depiction can allow for improved surgical and clinical outcomes.

Supplementary Material

Supplementary material is available at the *Journal of Breast Imaging* online.

Funding

This study was supported in part by multiple grants from the National Cancer Institute: P30-CA015704-40 (H.L., co-investigator), R01-CA203883 (H.R., principal investigator), R01-CA207290 (S.C.P., principal investigator), and U01-CA148131 (H.L., co-investigator).

Conflict of Interest Statement

The authors declare that they have no conflicts of interest directly related to this work. The authors disclose the following relationships not related to this work: H.R., MD, research grant support from GE

Healthcare and uncompensated consultant for Philips Healthcare; J.M.L., MD, MSc, research grant support from GE Healthcare; S.C.P., PhD, research grant support from GE Healthcare; D.S.H., research support from GE Healthcare, Philips Healthcare, Canon Medical Systems USA, and Siemens Healthineers; H.L., MD, research support from Zionexa and research grant support from Zeno Pharmaceuticals, Inc., and Sanofi-Aventis U.S.

References

- Findlay-Shirras LJ, Lima I, Smith G, Clemons M, Arnaout A. Population trends in lobular carcinoma of the breast: the Ontario experience. *Ann Surg Oncol* 2020;27(12):4711–4719.
- Luveta J, Parks RM, Heery DM, Cheung KL, Johnston SJ. Invasive lobular breast cancer as a distinct disease: implications for therapeutic strategy. *Oncol Ther* 2020;8(1):1–11.
- Schnitt SJ, Guidi AJ. Pathology of invasive breast cancer. In: Harris JR, Morrow M, Osborne CK, et al., eds. *Diseases of the Breast*. 3rd ed. Philadelphia, PA: Lippincott, Williams & Wilkins, 2004.
- Qureshi HS, Linden MD, Divine G, Raju UB. E-cadherin status in breast cancer correlates with histologic type but does not correlate with established prognostic parameters. *Am J Clin Pathol* 2006;125(3):377–385.
- Sprague BL, Arao RF, Miglioretti DL, et al; Breast Cancer Surveillance Consortium. National performance benchmarks for modern diagnostic digital mammography: update from the breast cancer surveillance consortium. *Radiology* 2017;283(1):59–69.
- Lehman CD, Arao RF, Sprague BL, et al. National performance benchmarks for modern screening digital mammography: update from the breast cancer surveillance consortium. *Radiology* 2017;283(1):49–58.
- Lopez JK, Bassett LW. Invasive lobular carcinoma of the breast: spectrum of mammographic, US, and MR imaging findings. *Radiographics* 2009;29(1):165–176.
- Caramella T, Chapellier C, Ettore F, Raoust I, Chamorey E, Balu-Maestro C. Value of MRI in the surgical planning of invasive lobular breast carcinoma: a prospective and a retrospective study of 57 cases: comparison with physical examination, conventional imaging, and histology. *Clin Imaging* 2007;31(3):155–161.
- Mann RM, Veltman J, Barentsz JO, Wobbes T, Blickman JG, Boetes C. The value of MRI compared to mammography in the assessment of tumour extent in invasive lobular carcinoma of the breast. *Eur J Surg Oncol* 2008;34(2):135–142.
- Parvaiz MA, Yang P, Razia E, et al. Breast MRI in invasive lobular carcinoma: a useful investigation in surgical planning? *Breast J* 2016;22(2):143–150.
- Mann RM. The effectiveness of MR imaging in the assessment of invasive lobular carcinoma of the breast. *Magn Reson Imaging Clin N Am* 2010;18(2):259–276.
- D’Orsi CJ, Sickles EA, Mendelson EB, et al. *ACR BI-RADS® Atlas, Breast Imaging Reporting and Data System*. Reston, VA: American College of Radiology; 2013.
- Rahbar H, Hippe DS, Alaa A, et al. The value of patient and tumor factors in predicting preoperative breast MRI outcomes. *Radiol Imaging Cancer* 2020;2(4):e190099. doi:10.1148/rycan.2020190099

14. Hortobagyi GN, Connolly JL, D'Orsi CJ, et al. Breast. In: Amin MB, Edge S, Greene F, et al., eds. *American Joint Committee on Cancer. AJCC Cancer Staging Manual*. 8th ed. New York, NY: Springer, 2017:589–636.
15. Grimsby GM, Gray R, Dueck A, et al. Is there concordance of invasive breast cancer pathologic tumor size with magnetic resonance imaging? *Am J Surg* 2009;198(4):500–504.
16. Luparia A, Mariscotti G, Durando M, et al. Accuracy of tumour size assessment in the preoperative staging of breast cancer: comparison of digital mammography, tomosynthesis, ultrasound and MRI. *Radiol Med* 2013;118(7):1119–1136.
17. Onesti JK, Mangus BE, Helmer SD, Osland JS. Breast cancer tumor size: correlation between magnetic resonance imaging and pathology measurements. *Am J Surg* 2008;196(6):844–848.
18. Lai HW, Chen DR, Wu YC, et al. Comparison of the diagnostic accuracy of magnetic resonance imaging with sonography in the prediction of breast cancer tumor size: a concordance analysis with histopathologically determined tumor size. *Ann Surg Oncol* 2015;22(12):3816–3823.
19. Mann RM, Hoogveen YL, Blickman JG, Boetes C. MRI compared to conventional diagnostic work-up in the detection and evaluation of invasive lobular carcinoma of the breast: a review of existing literature. *Breast Cancer Res Treat* 2008;107(1):1–14.
20. Dillon MF, Hill AD, Fleming FJ, et al. Identifying patients at risk of compromised margins following breast conservation for lobular carcinoma. *Am J Surg* 2006;191(2):201–205.
21. Gruber IV, Rueckert M, Kagan KO, et al. Measurement of tumour size with mammography, sonography and magnetic resonance imaging as compared to histological tumour size in primary breast cancer. *BMC Cancer* 2013;13:328. doi:10.1186/1471-2407-13-328
22. Pritt B, Ashikaga T, Oppenheimer RG, Weaver DL. Influence of breast cancer histology on the relationship between ultrasound and pathology tumor size measurements. *Mod Pathol* 2004;17(8):905–910.
23. Veltman J, Boetes C, van Die L, Bult P, Blickman JG, Barentsz JO. Mammographic detection and staging of invasive lobular carcinoma. *Clin Imaging* 2006;30(2):94–98.
24. Vijayaraghavan GR, Vedantham S, Santos-Nunez G, Hultman R. Unifocal invasive lobular carcinoma: tumor size concordance between preoperative ultrasound imaging and postoperative pathology. *Clin Breast Cancer* 2018;18(6):e1367–e1372.
25. Yeatman TJ, Cantor AB, Smith TJ, et al. Tumor biology of infiltrating lobular carcinoma. Implications for management. *Ann Surg* 1995;222(4):549–559.
26. Boetes C, Veltman J, van Die L, Bult P, Wobbes T, Barentsz JO. The role of MRI in invasive lobular carcinoma. *Breast Cancer Res Treat* 2004;86(1):31–37.
27. Muttalib M, Ibrahim R, Khashan AS, Hajaj M. Prospective MRI assessment for invasive lobular breast cancer. Correlation with tumour size at histopathology and influence on surgical management. *Clin Radiol* 2014;69(1):23–28.
28. Rodenko GN, Harms SE, Pruneda JM, et al. MR imaging in the management before surgery of lobular carcinoma of the breast: correlation with pathology. *AJR Am J Roentgenol* 1996;167(6):1415–1419.
29. Schelfout K, Van Goethem M, Kersschot E, et al. Preoperative breast MRI in patients with invasive lobular breast cancer. *Eur Radiol* 2004;14(7):1209–1216.
30. Truin W, Vugts G, Roumen RM, et al. Differences in response and surgical management with neoadjuvant chemotherapy in invasive lobular versus ductal breast cancer. *Ann Surg Oncol* 2016;23(1):51–57.
31. Fitzal F, Mittlboeck M, Steger G, et al. Neoadjuvant chemotherapy increases the rate of breast conservation in lobular-type breast cancer patients. *Ann Surg Oncol* 2012;19(2):519–526.
32. McLaughlin SA. Surgical management of the breast: breast conservation therapy and mastectomy. *Surg Clin North Am* 2013;93(2):411–428.
33. Singletary SE, Patel-Parekh L, Bland KI. Treatment trends in early-stage invasive lobular carcinoma: a report from the National Cancer Data Base. *Ann Surg* 2005;242(2):281–289.
34. Elmore JG, Nelson HD, Pepe MS, et al. Variability in pathologists' interpretations of individual breast biopsy slides: a population perspective. *Ann Intern Med* 2016;164(10):649–655.
35. Piper ML, Wong J, Fahrner-Scott K, et al. Success rates of re-excision after positive margins for invasive lobular carcinoma of the breast. *NPJ Breast Cancer* 2019;5:29. doi:10.1038/s41523-019-0125-7
36. Houssami N, Turner RM, Morrow M. Meta-analysis of pre-operative magnetic resonance imaging (MRI) and surgical treatment for breast cancer. *Breast Cancer Res Treat* 2017;165(2):273–283.